*The Canadian Mineralogist*
Vol. 57, pp. 215-223 (2019)
DOI: 10.3749/canmin.1800070

# WHITEITE-(MnMnMg), A NEW JAHNSITE-GROUP MINERAL FROM IRON MONARCH, SOUTH AUSTRALIA: DESCRIPTION AND CRYSTAL STRUCTURE

PETER ELLIOTT[§]

*Department of Earth Sciences, School of Physical Sciences, The University of Adelaide, Adelaide, South Australia 5005, Australia*
*South Australian Museum, North Terrace, Adelaide, South Australia 5000, Australia*

ANTHONY C. WILLIS

*Research School of Chemistry, The Australian National University, Canberra, Australian Capital Territory 2601, Australia*

## ABSTRACT

Whiteite-(MnMnMg), is a new jahnsite-group mineral found at the Iron Monarch Quarry, Iron Knob, South Australia, Australia, where it occurs associated with triploidite, rhodochrosite, and an unidentified Ca,Mn phosphate carbonate mineral. The new mineral occurs as a single unterminated, reddish, orange, prismatic crystal 1.2 mm in length and 0.3 mm across. The mineral is uniaxial (–), with $\alpha = 1.582(2)$, $\beta = 1.586(2)$, $\gamma = 1.613(2)$. The calculated $2V$ is 74.5°. The streak is pale orange. The luster is vitreous and the mineral is translucent. The mineral is brittle with an irregular fracture and a good cleavage parallel to {001}; its Mohs hardness is ~4. The measured specific gravity is 2.61(4) g/cm$^3$. The empirical formula, calculated on the basis of 26 O atoms per formula unit, is $(Mn^{2+}_{0.60},Ca_{0.41},Na_{0.03},K_{0.01})_{\Sigma 1.05}(Mn^{2+}_{0.92},Mg_{0.08})_{\Sigma 1.00}Mg_{2.00}(Al_{1.82},Mn^{3+}_{0.18})_{\Sigma 2.00}(PO_4)_{4.00}(OH)_{2.06}\cdot 7.95H_2O$. Whiteite-(MnMnMg) is monoclinic with space group $P2/a$; its unit-cell parameters are $a$ 15.0357(18), $b$ 6.9408(5), $c$ 9.9431(9) Å, $\beta$ 110.827(8)°, $V$ 969.86(16) Å$^3$, and $Z = 2$. The eight strongest lines in the X-ray powder diffraction pattern are [$d_{obs}$ Å ($I$) ($hkl$)]: 9.244(100)(001), 5.619(32)($\bar{1}1\bar{1}$), 4.839(20)(111, 20$\bar{2}$), 4.111(16)(1$\bar{1}\bar{2}$), 3.501(22)(3$\bar{1}\bar{2}$)(400, 020, 40$\bar{2}$), 2.936(16)(401), 2.759(30)(022,510), and 2.566(17)(42$\bar{1}$). The crystal structure has been refined from single-crystal X-ray data to $R = 0.0396$ for 23,703 unique observed reflections ($F_o > 4\sigma F_o$). The mineral is named for the chemical composition, in accordance with jahnsite group nomenclature.

*Keywords*: whiteite-(MnMnMg), new mineral species, jahnsite group, phosphate, crystal structure, Iron Monarch, Australia.

## INTRODUCTION

Minerals of the jahnsite group are most often found in phosphate-bearing granitic pegmatites where they occur as secondary minerals formed as a result of hydrothermal alteration of primary phosphates (Moore & Ito 1978, Roda *et al*. 2004). Less commonly, these minerals occur in deposits of sedimentary origin, *e.g.*, jahnsite-(CaFeMg) from Tom's quarry, South Australia (Elliott *et al*. 2014, Elliott 2016) and the subject of this paper, whiteite-(MnMnMg), from Iron Monarch, South Australia. Jahnsite was described as a new mineral species from the Tip Top pegmatite, near Custer, South Dakota by Moore (1974). The structure was published by Moore & Araki (1974). Whiteite was described as the Al analogue of jahnsite from the Lavra da Ilha pegmatite, Minas Gerais, Brazil by Moore & Ito (1978). Recognizing that a variety of cation substitutions were possible in the jahnsite structure type, Moore & Ito (1978) proposed a nomenclature scheme for the mineral group, generally referred to as the jahnsite group, with general formula $XM(1)M(2)_2M(3)_2(OH)_2(H_2O)_8(PO_4)_4$. Two subgroups were proposed, with occupancy of $M(3)$ by $Fe^{3+}$ for the jahnsites and by Al for the whiteites. The jahnsite group as well as the jahnsite and whiteite subgroups have been formally approved by the Commission on

§ *Corresponding author e-mail address*: peter.elliott@adelaide.edu.au

TABLE 1. COMPOSITIONAL DATA FOR WHITEITE-(MnMnMg)

| Constituent | wt.% | Range | Stand. Dev. |
|---|---|---|---|
| $Na_2O$ | 0.11 | 0.04–0.20 | 0.04 |
| CaO | 3.03 | 2.87–3.17 | 0.11 |
| $K_2O$ | 0.04 | 0.05–0.06 | 0.01 |
| $Al_2O_3$ | 12.10 | 11.76–12.47 | 0.23 |
| MgO | 10.97 | 10.64–11.46 | 0.24 |
| MnO** | 14.11 | 13.62–14.53 | 0.29 |
| $Mn_2O_3$** | 1.81 | 1.38–2.44 | 0.34 |
| $P_2O_5$ | 37.13 | 35.69–38.76 | 0.84 |
| $H_2O$ (calc)* | 21.15 | | |
| Total | 100.45 | | |

* $H_2O$ calculated from the crystal structure analysis.
** MnO and $Mn_2O_3$ contents are calculated assuming that the *M*1 sites are occupied by Mn, the *M*2 site is occupied by Mg and Mn, and the *M*3 sites are occupied by Al and $Mn^{3+}$.

TABLE 2. X-RAY POWDER DIFFRACTION DATA FOR WHITEITE-(MnMnMg)

| $I_{obs}$ | $d_{obs}$ | $I_{calc}$ | $d_{calc}$ | *h* | *k* | *l* |
|---|---|---|---|---|---|---|
| 100 | 9.244 | 100 | 9.293 | 0 | 0 | 1 |
| 4 | 6.921 | 1 | 6.910 | 2 | 0 | $\bar{1}$ |
| 8 | 6.250 | 3 | 6.223 | 1 | 1 | 0 |
| 32 | 5.619 | 19 | 5.594 | 1 | $\bar{1}$ | $\bar{1}$ |
| 14 | 4.930 | 3 | 4.938 | 2 | 1 | 0 |
| | | 2 | 4.897 | 2 | 1 | $\bar{1}$ |
| 20 | 4.839 { | 27 | 4.831 | 1 | 1 | 1 |
| | | 1 | 4.725 | 2 | 0 | $\bar{2}$ |
| 10 | 4.605 | 1 | 4.647 | 0 | 0 | 2 |
| 16 | 4.111 | 10 | 4.041 | 1 | $\bar{1}$ | $\bar{2}$ |
| 6 | 4.001 | 2 | 4.030 | 3 | 1 | $\bar{1}$ |
| 11 | 3.907 | 1 | 3.906 | 2 | $\bar{1}$ | $\bar{2}$ |
| 10 | 3.864 | 9 | 3.883 | 3 | 1 | 0 |
| 8 | 3.792 | 13 | 3.758 | 4 | 0 | $\bar{1}$ |
| | | 13 | 3.536 | 3 | $\bar{1}$ | $\bar{2}$ |
| 22 | 3.501 { | 4 | 3.513 | 4 | 0 | 0 |
| | | 6 | 3.471 | 0 | 2 | 0 |
| | | 6 | 3.455 | 4 | 0 | $\bar{2}$ |
| 11 | 3.262 | 11 | 3.258 | 3 | 1 | 1 |
| 14 | 3.125 | 10 | 3.098 | 0 | 0 | 3 |
| 16 | 2.936 | 26 | 2.957 | 4 | 0 | 1 |
| 11 | 2.899 | 20 | 2.888 | 4 | 0 | $\bar{3}$ |
| 6 | 2.877 | 6 | 2.869 | 3 | $\bar{1}$ | $\bar{3}$ |
| 30 | 2.759 | 32 | 2.781 | 0 | 2 | 2 |
| | | 4 | 2.605 | 5 | 1 | 0 |
| 17 | 2.566 | 13 | 2.550 | 4 | 2 | $\bar{1}$ |
| 8 | 2.341 | 3 | 2.344 | 6 | 1 | $\bar{1}$ |
| | | 3 | 2.331 | 6 | 1 | $\bar{2}$ |
| | | 3 | 2.298 | 1 | $\bar{1}$ | $\bar{4}$ |
| | | 3 | 2.072 | 1 | 1 | 4 |
| | | 3 | 1.998 | 4 | 0 | 3 |
| 3 | 1.962 | 3 | 1.955 | 4 | 0 | $\bar{5}$ |
| 4 | 1.936 | 6 | 1.931 | 0 | 2 | 4 |
| 6 | 1.885 | 17 | 1.879 | 8 | 0 | $\bar{2}$ |
| 4 | 1.735 | 9 | 1.735 | 0 | 4 | 0 |
| | | 4 | 1.567 | 8 | 2 | 0 |
| | | 5 | 1.549 | 0 | 0 | 6 |
| | | 3 | 1.547 | 8 | $\bar{2}$ | $\bar{4}$ |

New Minerals, Nomenclature and Classification (Kampf *et al.* 2019). Nineteen species are currently accepted as part of the jahnsite group, with $X$ = Ca, Na, Mn; $M(1)$ = Mn, $Fe^{2+}$; $M(2)$ = Mn, $Fe^{2+}$, Mg, $Fe^{3+}$; and $M(3)$ = Al, $Fe^{3+}$.

Whiteite-(MnMnMg) was found on a single specimen collected from the Iron Monarch quarry, Iron Knob, South Australia, Australia, in the late 1990s. The new mineral and name have been approved by the Commission on New Minerals, Nomenclature and Classification of the International Mineralogical Association (IMA 2015-092). Holotype material is preserved in the collection of the South Australian Museum, Adelaide, South Australia (Registration number G32398). Whiteite-(MnMnMg) has also been reported from the Jocão pegmatite, Minas Gerais, Brazil (Baijot *et al*. 2014) and from the Sapucaia mine Minas Gerais, Brazil (Baijot *et al*. 2012).

## Occurrence

Iron Monarch is the largest of several Precambrian sedimentary iron ore deposits located in the Middleback Ranges of South Australia. Mining in the Middleback Ranges commenced in 1900 and although mining at Iron Monarch ended in 1998, other deposits continue to produce iron ore for export and for smelting at Whyalla. The iron ore deposits are hosted by the Middleback Group, a sequence of Early Proterozoic chemical metasediments which are interpreted to have been deposited about 1950 to 1850 million years ago (Yeates 1990). Iron Monarch lies within a carbonate-facies iron formation, composed primarily of iron carbonate, silica, and iron oxide, with primary iron silicates such as iron-rich talc and cummingtonite–grunerite. Mineralogically, Iron Monarch is notable for an extensive suite of secondary phosphate and other oxysalt minerals (Francis 2010). The orebody contains pods of high-grade manganese ore and the presence of iron and manganese with small amounts of copper, zinc, bismuth, silver, phosphorous, arsenic, and other elements has led to an unusually diverse mineralogy, formed as a result of deep Tertiary and post-Tertiary weathering (Miles 1955).

Whiteite-(MnMnMg) was collected from a Mn-rich, carbonate-rich zone, comprising hematite, haus-

TABLE 3. CRYSTAL DATA, DATA COLLECTION, AND REFINEMENT DETAILS

| | |
|---|---|
| **Crystal data** | |
| Space group | *P*2/*a* |
| *a*, *b*, *c* (Å) | 15.0357(18), 6.9408(5), 9.9431(9) |
| β (°) | 110.827(8) |
| *V* (Å$^3$), Z | 969.86(16), 2 |
| *F*(000) | 757.0 |
| μ (mm$^{-1}$) | 1.712 |
| Absorption correction | multi-scan, $T_{min}$, $T_{max}$ = 0.82, 0.93 |
| Crystal dimensions (mm) | 0.11 × 0.07 × 0.02 |
| **Data collection** | |
| Diffractometer | Nonius KappaCCD |
| Temperature (K) | 293 |
| Radiation | Mo*K*α, λ = 0.71073 Å |
| Crystal detector distance (mm) | 40 |
| Rotation axis, width (°) | φ, ω 2.0 |
| Total number of frames | 281 |
| Collection time per degree (s) | 20 |
| θ range (°) | 2.899–30.219 |
| *h, k, l* ranges | –21 → 21, –9 → 9, –14 → 13 |
| Total reflections measured | 25,265 |
| Unique reflections | 2818 ($R_{int}$ = 0.0377) |
| **Refinement** | |
| Refinement on | $F^2$ |
| *R*1* for $F_o > 4\sigma(F_o)$ | 3.96% |
| w*R*2† for all $F_o^2$ | 12.14% |
| Reflections used $F_o^2 > 4\sigma(F_o^2)$ | 23703 |
| Number of parameters refined | 192 |
| GooF | 1.147 |
| $(\Delta/\sigma)_{max}$ | 0.000 |
| $\Delta\rho_{max}$, $\Delta\rho_{min}$ (e/Å) | 1.081, –0.697 |

*$R1 = \sum||F_o|-|F_c|| / \sum|F_o|$
†$wR2 = \sum w(|F_o|^2-|F_c|^2)^2 / \sum w|F_o|^2)^{1/2}$; $w = 1/[\sigma^2(F_o^2) + (0.042\ P)^2 + 12.60\ P]$; $P = ([\text{max of } (0 \text{ or } F_o^2)] + 2F_c^2)/3$

mannite, baryte, Mn-rich calcite, and rhodochrosite, on RL130 and RL120 in the north-eastern corner of the quarry (Francis 2010). Carbonate-rich veins host a number of secondary phosphate, arsenate, vanadate, and sulfate minerals which formed as late-stage, low-temperature hydrothermal phases (Pring *et al*. 1989, 1992, 2000). This suite of minerals includes two new mineral species, gatehouseite (Pring & Birch 1993) and waterhouseite (Pring *et al.* 2005).

An unusual feature of the secondary minerals from this zone is that many of them contain no Fe, even structures that would readily accommodate Fe, such as collinsite, fairfieldite, gatehouseite, arsenoclasite, tripoloidite, waterhouseite, and whiteite-(MnMnMg). This suggests that the source of the hydrothermal fluids from which these minerals crystallized was a region with a low concentration of Fe.

## Physical and Optical Properties

Whiteite-(MnMnMg) occurs as a single reddish orange, unterminated crystal 1.2 mm in length and 0.3 mm across. The crystal is prismatic along [100] in habit and shows forms {001} and {011}. The crystal is transparent, with vitreous luster and a white streak. The Mohs hardness is ~4, the tenacity is brittle, and the fracture is splintery. Density, measured by the sink float method using a sodium polytungstate-water mixture, is 2.61(4) g/cm$^3$. The calculated density is 2.632 g/cm$^3$ based on the empirical formula and 2.720 g/cm$^3$ based on the ideal formula. Optically, whiteite-(MnMnMg) is biaxial (–), with $\alpha = 1.582(2)$, $\beta = 1.586(2)$, $\gamma = 1.613(2)$ determined in white light. The calculated $2V$ is 74.5°. Pleochroism is distinct; *X* pale grey, *Y* orange-pink, *Z* beige, absorption $Y > Z > X$. A Gladstone-Dale calculation gave a compatibility index

TABLE 4. FRACTIONAL ATOMIC COORDINATES AND DISPLACEMENT PARAMETERS FOR WHITEITE-(MnMnMg)

| Atom | *x* | *y* | *z* | $U^{eq}$ | $U^{11}$ | $U^{22}$ | $U^{33}$ | $U^{12}$ | $U^{13}$ | $U^{23}$ |
|---|---|---|---|---|---|---|---|---|---|---|
| Mn (*X*) | 0.25 | 0.96332(11) | 0 | 0.0193(2) | 0.0191(4) | 0.0114(4) | 0.0208(4) | 0 | –0.0013(3) | 0 |
| Mn (*M*1) | 0.25 | 0.46379(10) | 0 | 0.0119(2) | 0.0134(3) | 0.0114(4) | 0.0128(4) | 0 | 0.0069(3) | 0 |
| Mg1 (*M*2a) | 0.5 | 0 | 0.5 | 0.0061(3) | 0.0058(6) | 0.0047(6) | 0.0072(6) | –0.0031(4) | 0.0015(5) | –0.0003(4) |
| Mg2 (*M*2b) | 0.25 | 0.50254(18) | 0.5 | 0.0053(3) | 0.0057(6) | 0.0058(6) | 0.0053(6) | 0 | 0.0030(5) | 0 |
| Al1 (*M*3a) | 0 | 0 | 0 | 0.0061(3) | 0.0067(5) | 0.0027(5) | 0.0096(6) | 0.0003(4) | 0.0037(4) | 0.0009(4) |
| Al2 (*M*3b) | 0 | 0.5 | 0 | 0.0053(3) | 0.0058(5) | 0.0025(5) | 0.0088(6) | 0.0004(4) | 0.0040(4) | 0.0008(4) |
| P1 | 0.17761(5) | 0.25464(10) | 0.18935(9) | 0.0120(2) | 0.0128(4) | 0.0117(4) | 0.0118(4) | –0.0005(3) | 0.0050(3) | 0.0003(3) |
| P2 | 0.08209(5) | 0.74881(10) | 0.80415(9) | 0.0111(2) | 0.0113(4) | 0.0110(4) | 0.0117(4) | 0.0019(3) | 0.0050(3) | 0.0012(2) |
| O1 | 0.26524(17) | 0.2062(4) | 0.1480(3) | 0.0260(6) | 0.0175(12) | 0.0400(15) | 0.0243(13) | 0.0092(11) | 0.0122(10) | 0.0107(10) |
| O2 | 0.20714(19) | 0.2949(3) | 0.3480(3) | 0.0222(5) | 0.0357(14) | 0.0168(11) | 0.0132(11) | –0.0028(9) | 0.0074(10) | –0.0013(10) |
| O3 | 0.10982(17) | 0.0832(3) | 0.1505(3) | 0.0244(5) | 0.0259(12) | 0.0102(10) | 0.0262(13) | 0.0023(9) | –0.0043(10) | –0.0029(9) |
| O4 | 0.13398(14) | 0.4327(3) | 0.0933(2) | 0.0143(4) | 0.0140(10) | 0.0101(10) | 0.0187(11) | 0.0012(8) | 0.0055(8) | –0.0008(7) |
| O5 | 0.18921(15) | 0.6944(3) | 0.8555(2) | 0.0184(5) | 0.0130(10) | 0.0241(12) | 0.0177(12) | 0.0038(9) | 0.0048(9) | 0.0033(8) |
| O6 | 0.04660(16) | 0.7830(3) | 0.6426(2) | 0.0170(5) | 0.0190(11) | 0.0177(11) | 0.0128(11) | 0.0043(8) | 0.0039(9) | 0.0021(8) |
| O7 | 0.08062(16) | 0.9323(3) | 0.8916(3) | 0.0191(5) | 0.0285(12) | 0.0103(10) | 0.0245(12) | –0.0002(9) | 0.0168(10) | –0.0028(8) |
| O8 | 0.02511(15) | 0.5859(3) | 0.8379(2) | 0.0152(4) | 0.0207(11) | 0.0100(10) | 0.0182(11) | 0.0003(8) | 0.0109(9) | –0.0003(8) |
| OH9 | 0.02159(15) | 0.7501(3) | 0.0851(2) | 0.0124(4) | 0.0141(10) | 0.0080(9) | 0.0153(11) | 0.0001(7) | 0.0054(9) | –0.0003(7) |
| OW10 | 0.22716(19) | 0.7279(4) | 0.3441(3) | 0.0249(6) | 0.0343(15) | 0.0242(13) | 0.0215(13) | 0.0035(10) | 0.0163(12) | 0.0075(10) |
| OW11 | 0.4464(2) | 0.2178(4) | 0.3433(3) | 0.0308(7) | 0.0395(16) | 0.0164(12) | 0.0226(14) | –0.0008(10) | –0.0059(12) | –0.0034(11) |
| OW12 | 0.63093(18) | 0.9986(4) | 0.4694(3) | 0.0260(6) | 0.0222(13) | 0.0222(13) | 0.0368(16) | –0.0126(11) | 0.0143(12) | –0.0055(10) |
| OW13 | 0.39149(18) | 0.5151(4) | 0.5129(3) | 0.0221(6) | 0.0174(11) | 0.0179(12) | 0.0314(15) | 0.0050(10) | 0.0092(10) | –0.0002(9) |
| H10a | 0.234(4) | 0.725(7) | 0.263(6) | 0.05 | | | | | | |
| H11a | 0.391(4) | 0.198(7) | 0.270(6) | 0.05 | | | | | | |
| H11b | 0.422(3) | 0.316(7) | 0.384(6) | 0.05 | | | | | | |
| H12a | 0.648(3) | 0.905(7) | 0.433(6) | 0.05 | | | | | | |
| H12b | 0.675(4) | 1.053(7) | 0.528(6) | 0.05 | | | | | | |
| H13a | 0.414(3) | 0.601(7) | 0.473(6) | 0.05 | | | | | | |
| H13b | 0.423(4) | 0.473(8) | 0.581(6) | 0.05 | | | | | | |

TABLE 5. SELECTED INTERATOMIC DISTANCES (Å) AND HYDROGEN BONDS FOR WHITEITE-(MnMnMg)

| | | | | | |
|---|---|---|---|---|---|
| Mn (*X*) | O1 | 2.196(3) ×2 | Al2 (*M*3a) | O3 | 1.882(2) ×2 |
| | O5 | 2.334(2) ×2 | | OH9 | 1.907(2) ×2 |
| | O7 | 2.396(2) ×2 | | O7 | 1.945(2) ×2 |
| | O3 | 3.101(2) ×2 | | <Al–O> | 1.911 |
| | <Mn–O> | 2.507 | | | |
| | | | Al3 (*M*3b) | O8 | 1.879(2) ×2 |
| Mn (*M*1) | O5 | 2.128(2) ×2 | | OH9 | 1.908(2) ×2 |
| | O4 | 2.258(2) ×2 | | O4 | 1.951(2) ×2 |
| | O1 | 2.275(3) ×2 | | <Al–O> | 1.913 |
| | <Mn–O> | 2.261 | | | |
| | | | P1 | O2 | 1.506(2) |
| Mg1 (*M*2a) | O6 | 2.016(2) ×2 | | O3 | 1.524(2) |
| | OW12 | 2.096(3) ×2 | | O1 | 1.550(2) |
| | OW11 | 2.114(3) ×2 | | O4 | 1.557(2) |
| | <Mg–O> | 2.075 | | <P–O> | 1.534 |
| Mg2 (*M*2b) | O2 | 2.020(2) ×2 | P2 | O6 | 1.521(2) |
| | OW13 | 2.087(3) ×2 | | O8 | 1.526(2) |
| | OW10 | 2.142(3) ×2 | | O7 | 1.547(2) |
| | <Mg–O> | 2.083 | | O5 | 1.553(2) |
| | | | | <P–O> | 1.537 |
| Hydrogen bonds | | | | | |
| *D*–H···*A* | *D*–H | H···*A* | *D*···*A* | ∠*D*–H···*A* | |
| OW10–H10a···O5$^{i}$ | 0.85(5) | 1.94(5) | 2.711(3) | 152(5) | |
| OW11–H11a···O1$^{ii}$ | 0.90(5) | 1.85(5) | 2.727(4) | 164(5) | |
| OW12–H12a···O2$^{ii}$ | 0.825(5) | 1.993(5) | 2.811(4) | 171(5) | |
| OW13–H13a···O6$^{i}$ | 0.85(5) | 1.93(5) | 2.781(4) | 172(5) | |
| OW13–H13b···O6$^{iv}$ | 0.74(5) | 2.49(5) | 3.040(3) | 134(5) | |

Symmetry codes: (i) $-x+1/2$, $y$, $-z+1$; (ii) $x$, $y$, $z$; (iii) $-x+1$, $-y+2$, $-z+1$; (iv) $x+1/2$, $-y+1$, $z$.

of 0.003, which is classed as superior (Mandarino 1981).

## Chemical Composition

Chemical analyses (12) were carried out using a Cameca SXFive electron microprobe (WDS mode, 15 kV, 10 nA, beam diameter 20 μm) (Table 1). The following standards and X-ray lines were used: albite (Na*K*α, Al*K*α), plagioclase (Ca*K*α), almandine–pyrope (Fe*K*α, Mg*K*α), rhodonite (Mn*K*α), sanidine (K*K*α), and apatite (P*K*α). No other element with atomic number ≥9 was detected in amounts >0.05 wt.% oxide. There was no evidence of chemical zoning with variable composition in the analyzed crystal as is common for jahnsite group minerals (Kampf *et al.* 2008, Grey *et al.* 2010, Capitelli *et al.* 2011). Results were processed using the φ(ρZ) correction procedure of Pouchou & Pichoir (1985). The small amount of material available did not allow for the direct determination of $H_2O$ so it was calculated based on the structure determination. Using the approach for cation assignments recommended by Moore & Ito (1978) gives an empirical formula (based on 26 O *apfu*) of $(Mn^{2+}_{0.60},Ca_{0.41},Na_{0.03},K_{0.01})_{\Sigma 1.05}(Mn^{2+}_{0.92},Mg_{0.08})_{\Sigma 1.00}Mg_{2.00}(Al_{1.82},Mn^{3+}_{0.18})_{\Sigma 2.00}(PO_4)_{4.00}(OH)_{2.06}\cdot 7.95H_2O$.

## X-ray Powder Diffraction

Powder X-ray diffraction data (Table 2) were collected using a Rigaku Hiflux Homelab diffractometer (Cu*K*α X-radiation, $\lambda = 1.541870$ Å). Calculated intensities were obtained from the structure model using the program UnitCell (Holland & Redfern 1997). The unit-cell parameters, refined using the least-squares method as implemented in the program UnitCell, are $a$ 15.010(3), $b$ 6.949(2), $c$ 9.986(1) Å, $\beta = 111.09(2)°$, $V = 971.9(2)$ Å$^3$.

## Structure Determination

A crystal fragment of dimensions 0.11 × 0.07 × 0.02 mm was mounted on a glass fiber and X-ray intensity data were collected at room temperature using a Nonius KappaCCD diffractometer. The measured intensities were corrected for Lorentz and polarization effects (Otwinowski & Minor 1997, Otwinowski *et al.* 2003). An absorption correction was applied using the Gaussian integration method

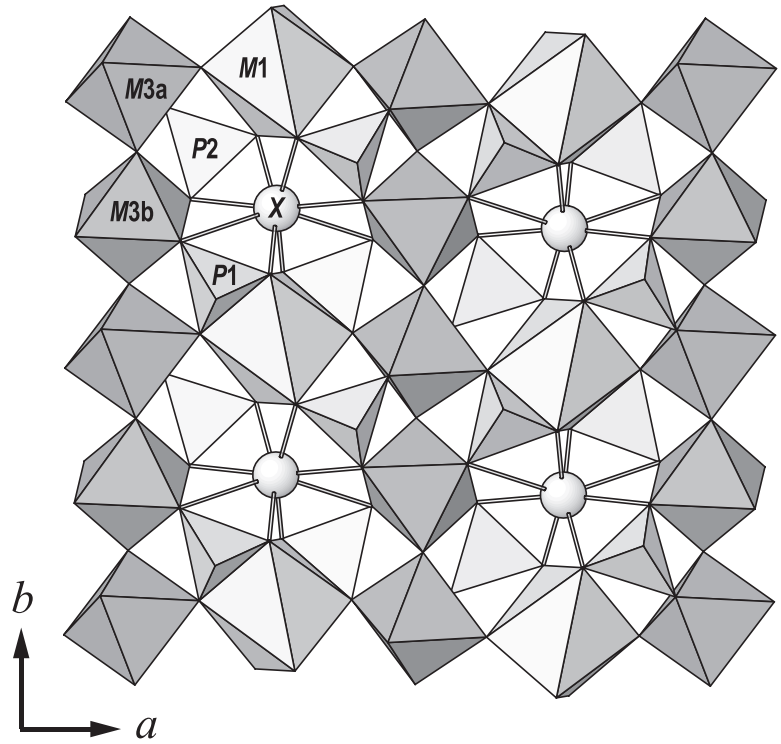


FIG. 1. The crystal structure of whiteite-(MnMnMg) viewed in a direction close to {001}. All structure drawings were completed using ATOMS (Dowty 1999).

(Coppens 1970), with minimum and maximum transmission-coefficients of 0.824 and 0.929, respectively. The unit cell-parameters, refined with the program HKL-SCALEPACK, are $a = 15.0357(18)$, $b = 6.9408(5)$, $c = 9.9431(9)$ Å, $\beta = 110.827(8)°$, $V = 969.86(16)$ Å$^3$. Conditions for the data collection and subsequent refinement are summarized in Table 3. Structure refinement was initiated in space group $P2/a$ using the coordinates of Moore & Araki (1974) and refined using SHELXL-97 (Sheldrick 2015) within the WinGX program suite (Farrugia 2012). The $R$ index converged to a value of 5.56%. Examination of diffraction images indicated that the crystal was twinned as shown by splitting of diffraction spots, as is commonly reported for jahnsite-group minerals. Application of ROTAX (Cooper *et al.* 2002) showed that twinning was due to 180° rotation about [100], twin law $\left[1\ 0\ 0/0\ \overline{1}\ 0/\overline{0.47}\ 0\ \overline{1}\right]$. A SHELX HKLF 5 reflection file was created and refinement resulted in refined twin components of 0.14:0.86 and $R1 = 4.31\%$. The positions of five of the H atoms belonging to $H_2O$ groups were located in the difference Fourier maps;

TABLE 6. REFINED SITE-SCATTERING VALUES (*epfu*) AND ASSIGNED SITE-POPULATIONS FOR WHITEITE-(MnMnMg)

| Site | | Site scattering | Site population (from the chemical analysis) | Calculated site scattering | $<M\text{–}O>_{obs}$ | $<M\text{–}O>_{calc}$ |
|---|---|---|---|---|---|---|
| *X* | | 22.15 | $Mn_{0.57}Ca_{0.39}Na_{0.03}K_{0.01}$ | 22.81 | 2.506 | 2.308 |
| *M*1 | Mn1 | 23.18 | $Mn^{2+}_{0.92}Mg^{3+}_{0.08}$ | 23.96 | 2.219 | 2.181 |
| *M*2 | Mg1 | 12.96 | $Mg_{1.00}$ | 12.00 | 2.079 | 2.077 |
| | Mg2 | 12.96 | $Mg_{1.00}$ | 12.00 | 2.085 | 2.077 |
| *M*3 | Al2 | 14.20 | $Al_{0.91}Mn^{3+}_{0.09}$ | 14.08 | 1.912 | 1.892 |
| | Al3 | 13.65 | $Al_{0.91}Mn^{3+}_{0.09}$ | 14.08 | 1.914 | 1.898 |

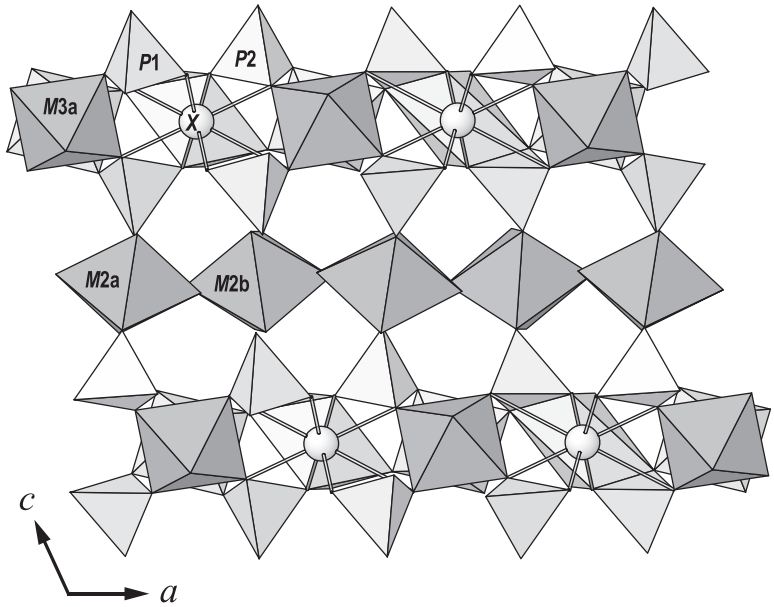


FIG. 2. The crystal structure of whiteite-(MnMnMg) viewed along [010].

the remaining H atoms could not be located. The H sites were refined with soft restraints of 0.82(3) Å on the O–H distances and isotropic displacement parameters were held constant at 0.05. The final cycle of the refinement converged to $R1 = 3.96\%$ for a model including anisotropic displacement parameters for all non-H atoms. The atomic positional parameters and anisotropic displacement parameters are given in Table 4, selected interatomic distances are given in Table 5, refined site-scattering values and assigned populations for selected sites in Table 6, and the result of the bond-valence analysis is given in Table 7.

The structure of the jahnsite group minerals is based on chains of trans corner-sharing $[M3O_4(OH)_2]$ octahedra that extend in the **b**-direction and are decorated by bridging ($PO_4$) groups (Fig. 1). The chains are linked *via* *X* site polyhedra and *M*1 octahedra into layers parallel to (001) (Fig. 2). The layers are linked *via* $[M2O_2(H_2O)_4]$ octahedra into a three dimensional structure. The *X* site is coordinated by eight O atoms with a square antiprism geometry. The coordination is more irregular than that in the structures of other whiteites, with six short bond distances of 2.196 to 2.396 Å and two long bond distances of 3.101 Å. Calculation of the bond-length distortion (BLD) coefficient (Renner & Lehmann 1986) gives a value of 11.885, indicating the degree of bond length distortion is more pronounced than in whiteite-(CaFeMg) (Capitelli *et al.* 2011), whiteite-(CaMnMn) (Grey *et al.* 2010), and whiteite-(CaMnMn) (Yakovenchuk *et al.* 2012) with values of 5.969, 7.909, and 8.088, respectively. The *X* site has a refined occupancy of 22.15 $e^-$ per formula unit, which matches 22.57 $e^-$ from the electron microprobe analyses (Table 6). Coordination of the *M*2 and *M*3 sites is similar to those in the structures of other whiteites, with similar mean bond distances. The $M1O_6$ octahedron is strongly distorted, with intra-octahedral angles deviating by up to 25.2° from ideal angles, whereas the $M2O_6$ and $M3O_6$ octahedra show only minor distortion. The site scattering of 23.18 $e^-$ and mean bond length (Table 5) at *M*1 are compatible with occupancy of this site by $Mn^{2+}$ plus minor Mg. Refinement of the occupancy of the *M*2 sites (12.96 $e^-$ and 12.00 $e^-$ for *M*2a and *M*2b, respectively) shows complete occupancy by Mg with possible minor Mn at *M*2a. The observed <M–O> lengths (Table 5), however, suggest minor Mn at *M*2b. The *M*3 sites are coordinated by four O atoms and two OH groups. The *M*3b site shows slightly greater bond-length distortion than the *M*3a site and has a refined site-scattering value of 14.04 *epfu* compared to 15.21 *epfu* for the *M*3b site. This suggests greater substitution of $Mn^{3+}$ for Al at the *M*3b site. The *M*3 sites show greater bond length distortion than in other whiteites, which is attributed to the presence of $Mn^{3+}$.

For the H atoms located during the refinement, the hydrogen bonding scheme (Table 6) is identical to that

TABLE 7. BOND VALENCE (*vu*) TABLE FOR WHITEITE-(MnMnMg)

| | Mn (*X*) ×2 ↓ | Mn (*M*1) ×2 ↓ | Mg1 (*M*2a) ×2 ↓ | Mg2 (*M*2b) ×2 ↓ | Al2 (*M*3a) ×2 ↓ | Al3 (*M*3b) ×2 ↓ | P1 | P2 | H9 | H10a | H10b | H11a | H11b | H12a | H12b | H13a | H13b | Sum |
|---|---|---|---|---|---|---|---|---|---|---|---|---|---|---|---|---|---|---|
| O1 | 0.40 | 0.27 | | | | | 1.20 | | | | | 0.20 | | | | | | 2.07 |
| O2 | | | | 0.40 | | | 1.34 | | | | | | | 0.17 | | | | 1.91 |
| O3 | 0.04 | | | | 0.55 | | 1.29 | | | | | | | | | | | 1.88 |
| O4 | | 0.28 | | | | 0.46 | 1.18 | | | | | | | | | | | 1.92 |
| O5 | 0.29 | 0.39 | | | | | | 1.20 | | 0.20 | | | | | | | | 2.08 |
| O6 | | | 0.40 | | | | | 1.30 | | | | | | | | | 0.10 | 1.80 |
| O7 | 0.25 | | | | 0.46 | | | 1.21 | | | | | | | | | | 1.92 |
| O8 | | | | | | 0.56 | | 1.28 | | | | | | | | | | 1.84 |
| OH9 | | | | | 0.52 | 0.51 | | | 0.99 | | | | 0.01 | | | | | 2.03 |
| OW10 | | | | 0.30 | | | | | | 0.80 | 1.00 | | | | 0.12 | | | 2.22 |
| OW11 | | | 0.32 | | | | | | 0.01 | | | 0.80 | 0.99 | | | | | 2.12 |
| OW12 | | | 0.33 | | | | | | | | | | | 0.83 | 0.88 | | | 2.04 |
| OW13 | | | | 0.34 | | | | | | | | | | | | 1.00 | 0.90 | 2.24 |
| Sum | 1.96 | 1.88 | 2.10 | 2.08 | 3.06 | 3.06 | 5.01 | 4.99 | 1.00 | 1.00 | 1.00 | 1.00 | 1.00 | 1.00 | 1.00 | 1.00 | 1.00 | |

Bond strengths based upon cation site occupancies. Bond valence parameters are from Gagné & Hawthorne (2015). Hydrogen-bond strengths are based on O–O bond lengths from Brown & Altermatt (1985).

for whiteite-(CaFeMg) (Capitelli *et al.* 2011). The remaining hydrogen bonds identified by Capitelli *et al*. (2011) also likely occur in whiteite-(MnMnMg) on the basis of stereochemical considerations and D···A distances. All hydrogen bonds are weak to moderately strong in strength.

## Acknowledgments

Ben Wade of Adelaide Microscopy, The University of Adelaide, is thanked for assistance with the microprobe analysis. The specimen containing whiteite-(MnMnMg) was kindly provided by Glynn Francis. Reviewers Anthony Kampf and Nicola Rotiroti and Associate Editor Pietro Vignola are thanked for their constructive comments on the manuscript.

## References

Baijot, M., Hatert, F., & Philippo, S. (2012) Mineralogy and geochemistry of phosphates and silicates in the Sapucaia pegmatite, Minas Gerais, Brazil: Genetic implications. *Canadian Mineralogist* **50**, 1531–1554.

Baijot, M., Hatert, F., Dal Bo, F., & Philippo, S. (2014) Mineralogy and petrography of phosphate mineral associations from the Jocão pegmatite, Minas Gerais, Brazil. *Canadian Mineralogist* **52**, 373–397.

Brown, I.D. & Altermatt, D. (1985) Bond-valence parameters obtained from a systematic analysis of the inorganic crystal structure database. *Acta Crystallographica* **B41**, 244–247.

Capitelli, F., Chita, G., Cavallo, A., Bellatreccia, F., & Ventura, G.D. (2011) Crystal structure of whiteite-(CaFeMg) from Crosscut Creek, Canada, *Zeitschrift für Kristallographie* **226**, 731–738.

Cooper, R.I., Gould, R.O., Parsons, S., & Watkin, D.J. (2002) The derivation of non-merohedral twin laws during refinement by analysis of poorly fitting intensity data and the refinement of non-merohedrally twinned crystal structures in the program CRYSTALS. *Journal of Applied Crystallography* **35**, 168–174.

Coppens, P. (1970) *Crystallographic Computing* (F.R. Ahmed, S.R. Hall, & C.P. Huber, eds.). Munksgaard, Copenhagen, Denmark (255–270).

Dowty, E. (1999) *ATOMS for Windows and Macintosh*. Version 5.0.6. Shape Software, Kingsport, Tennessee, United States.

Elliot, P. (2016) Jahnsite-(CaFeMg), a new mineral from Tom's quarry, South Australia: Description and crystal structure. *European Journal of Mineralogy* **28**, 991–996.

Elliott, P., Peisley, V.S., & Mills, S. (2014) The Phosphate Deposits of South Australia. *Australian Journal of Mineralogy* **17**, 3–32.

Farrugia, L.J. (2012) WinGX and ORTEP for Windows: an update. *Journal of Applied Crystallography* **45**, 849–854.

Francis, G.L. (2010) *Minerals of Iron Monarch*. OneSteel, Whyalla, South Australia, 165 pp.

Gagné, O.C. & Hawthorne, F.C. (2015) Comprehensive derivation of bond-valence parameters for ion pairs involving oxygen. *Acta Crystallographica* **B71**, 562–578.

Grey, I.E., Mumme, W.G., Neville, S.M., Wilson, N.C., & Birch, W.D. (2010) Jahnsite-whiteite solid solutions and associated minerals in the phosphate pegmatite at Hagendorf-Süd, Bavaria, Germany. *Mineralogical Magazine* **74**, 969–978.

Holland, T.J.B. & Redfern, S.A.T. (1997) Unit cell refinement from powder diffraction data: the use of regression diagnostics. *Mineralogical Magazine* **61**, 65–77.

Kampf, A.R., Steele, I.M., & Loomis, Th.A. (2008) Jahnsite-(NaFeMg), a new mineral from the Tip Top mine, Custer County, South Dakota: Description and crystal structure. *American Mineralogist* **93**, 940–945.

Kampf, A.R., Alves, P., Kasatkin, A., & Škoda, R. (2019) Jahnsite-(MnMnZn), a new jahnsite-group mineral, and formal approval of the jahnsite group. *European Journal of Mineralogy* (in press).

Mandarino, J.A. (1981) The Gladstone-Dale relationship: Part IV: The compatibility concept and its application. *Canadian Mineralogist* **19**, 441–450.

Miles, K.R. (1955) The geology and iron ore resources of the Middleback Range Area. *Bulletin of the Geological Survey of South Australia* **33**, 245 pp.

Moore, P.B. (1974) I. Jahnsite, segelerite, and robertsite, three new transition metal phosphate species. II. Redefinition of overite, an isotype of segelerite. III. Isotypy of robertsite, mitridatite, and arseniosiderite. *American Mineralogist* **59**, 48–59.

Moore, P.B. & Araki, T. (1974) Jahnsite, $CaMn^{2+}Mg_2(H_2O)_8Fe_2^{3+}(OH)_2[PO_4]_4$: A novel stereoisomerism of ligands about octahedral corner-chains. *American Mineralogist* **59**, 964–973.

Moore, P.B. & Araki, T. (1978) I. Whiteite, a new species, and a proposed nomenclature for the jahnsite–whiteite complex series. II. New data on xanthoxenite. III. Salmonsite discredited. *Mineralogical Magazine* **42**, 309–323.

Otwinowski, Z. & Minor, W. (1997) Processing X-ray diffraction data collected in oscillation mode. *In* Macromolecular Crystallography **276** (C.W. Carter Jr. & R.M. Sweet, eds.). Academic Press, New York, United States (307–326).

Otwinowski, Z., Borek, D., Majewski, W., & Minor, W. (2003) Multiparametric scaling of diffraction intensities. *Acta Crystallographica* **A59**, 228–234.

Pouchou, J.L. & Pichoir, F. (1985) "PAP" $\phi$ ($\rho$Z) procedure for improved quantitative microanalysis. *In* Microbeam Analysis (J.T. Armstrong, ed.). San Francisco Press, San Francisco, California, United States (104–106).

Pring, A. & Birch, W.D. (1993) Gatehouseite, a new manganese hydroxy phosphate from Iron Monarch, South Australia. *Mineralogical Magazine* **57**, 309–313.

Pring, A., Francis, G., & Birch, W.D. (1989) Pyrobelonite, arsenoklasite, switzerite and other recent finds at Iron Monarch, South Australia. *Australian Mineralogist* **4**, 49–55.

Pring, A., Francis, G., & Birch, W.D. (1992) Nissonite, namibite, and other additions to the mineral suite from Iron Monarch, South Australia. *Australian Mineralogist* **6**, 31–39.

Pring, A., Kolitsch, U., & Francis, G. (2000) Additions to the mineralogy of the Iron Monarch deposit, Middleback Ranges, South Australia. *Australian Journal of Mineralogy* **6**, 9–23.

Pring, A., Kolitsch, U., & Birch, W.D. (2005) Description and unique crystal structure of waterhouseite, a new hydroxy manganese phosphate species from the Iron Monarch deposit, Middleback Ranges, South Australia. *Canadian Mineralogist* **43**, 1401–1410.

Renner, B. & Lehmann, G. (1986) Correlation of angular and bond length distortions in $TO_4$ units in crystals. *Zeitschrift für Kristallographie* **175**, 43–59.

Roda, E., Pesquera, A., Fontan, F., & Keller, P. (2004) Phosphate mineral associations in the Cañada pegmatite (Salamanca, Spain): paragenetic relationships, chemical compositions, and implications for pegmatite evolution. *American Mineralogist* **89**, 110–125.

Sheldrick, G.M. (2015) Crystal Structure Refinement with SHELXL. *Acta Crystallographica* **C71**, 3–8.

Yakovenchuk, V.N., Keck, E., Krivovichev, S.V., Pakhomovsky, Y.A., Selivanova, E.A., Mikhailova, J.A., Chernyatieva, A.P., & Ivanyuk, G.Yu. (2012) Whiteite-(CaMnMn), $CaMnMn_2Al_2[PO_4]_4(OH)_2{\cdot}8H_2O$, a new mineral from the Hagendorf-Süd granitic pegmatite, Germany. *Mineralogical Magazine* **76**, 2761–2771.

Yeates, G. (1990) Middleback Range iron ore deposits. *In* Geology of the Mineral Deposits of Australia and Papua New Guinea (F.E. Hughes, ed.). The Australasian Institute of Mining and Metallurgy, Melbourne, Australia (1045–1048).

*Received December 2, 2018. Revised manuscript accepted February 2, 2019.*